

STAMPING OF HIGH PERFORMANCE THERMOPLASTIC COMPOSITES FOR THE AUTOMOTIVE INDUSTRY

David Trudel-Boucher
National Research Council Canada, Advanced Polymer Composites,
Boucherville (Qc), Canada
david.trudel-boucher@cnrc-nrc.gc.ca

Keywords: *Continuous Fiber Thermoplastic Composites, Stamping, Automotive*

ABSTRACT

In this study, an experimental investigation was performed to evaluate the potential of thermoplastic composites to be used for the fabrication of an automotive intrusion beam using the composite stamping process. To assess the potential of this technology, mechanical properties of several high performance thermoplastic composite materials were first determined on coupons. From these tests, most promising materials for the fabrication of a composite intrusion beam were found to be GF/PP and CF/PA66 laminates due to the balance of strength and deformation obtained for these materials. Then, stamped composite components were manufactured from GF/PP and CF/PA66 laminates and tested under three-point flexural loading. Load-displacement curves obtained for these composites were then compared to requirements for side impact protection. Results showed that sufficient strength could be achieved, thus demonstrating the potential of stamped thermoplastic composites to be used for the fabrication of structural automotive components.

1 INTRODUCTION

In recent years, there has been increasing interest for the use of high performance polymer composites in the automotive industry to achieve weight reduction that cannot be obtained with metals. As proof of this growing interest, several strategic alliances have been developed between OEM's and carbon fiber suppliers (i.e. BMW with SGL Group, GM with Toho Tenax, Daimler with Toray, Ford with DowAska and Jaguar Land Rover with Cytec) [1]. Market research also show that composite usage in automotive applications will continue to grow significantly in the upcoming years, certain research predicting compound annual growth rate of up to 10% until 2020 [2]. Main driver for the integration of composites in the automotive industry is the Corporate Fuel Average Efficiency (CAFE) regulation that requires fuel consumption of 54.5 mpg (4.3 L/100 km) to be reached by 2025. According to one study [3], the use of lightweight materials such as composites can result in significant fuel consumption reduction along with enormous environmental benefits: trimming the weight of a vehicle by 1 kg resulting in a 17-20 kg reduction in the amount of CO₂ emitted during the lifetime of that vehicle. Study from Oak Ridge National Laboratory also showed that replacing today's steel body-in-white (BIW) with an integrated carbon fiber composite structure could result in a 60 percent mass reduction, boosting fuel efficiency by as much as 30 percent [4]. This offers significant potential not only for meeting new fuel-economy standards with conventional engines, but also to offset added weight from electric battery packs, fuel-cell storage cylinders and other equipment essential to alternative-powertrain vehicles. However, most manufacturing process adapted to high performance composites do not meet the cycle time targeted by the automotive industry for the production of large series.

One of the most promising processes to cost-efficiently manufacture high performance composite parts for the automotive industry is the composite stamping process, a process similar to the widely used metal stamping process. One of the key advantages of this technology is the potential to manufacture light weight automotive parts in very short cycle times from continuous fiber thermoplastic composites. In addition, the composite stamping process also offer the potential of being implemented using infrastructure already in place, since forming presses are commonly used in the automotive industry. Although this process has been used in the aerospace sector to manufacture parts such as brackets and stringers for several years, little work has been done to date on automotive applications. Therefore, significant work still remains to be done in order to adapt the composite stamping process to the requirements of the automotive industry.

In this study, an experimental investigation on stamping of an automotive composite intrusion beam is conducted. This component was selected because of the challenges associated to the balance of stiffness, strength and deformation that must be achieved to meet the requirements. In order to evaluate the potential of high performance thermoplastic composites to be used for the fabrication of such structural part, the mechanical behavior of several high performance composite materials was first investigated by performing flexural tests on coupons. From these small scale tests, most-promising composite configurations were identified. Then, stamping trials were conducted to manufacture full-scale intrusion beams based on the results obtained from small-scale tests. Finally, flexural tests were conducted on full-scale stamped components to study their mechanical behavior and to compare results with side impact requirements.

2 EXPERIMENTAL PROCEDURES

2.1 Materials

Four continuous fiber thermoplastic composite materials were investigated in this study. These materials consist of glass fiber/polypropylene (GF/PP), glass fiber/polyamide 6 (GF/PA6), carbon fiber/polyamide 6 (CF/PA6) and carbon fiber/polyamide 66 (CF/PA66) composites. All of these materials are commercially available in the form of pre-impregnated tapes. Table 1 shows the fiber content and recommended processing temperatures for the investigated materials.

Table 1. Studied continuous fiber thermoplastic composites.

Materials	Fiber content (Wt. %)	Recommended processing temperatures (°C)
GF/PP	70	204
GF/PA6	60	271
CF/PA6	60	249-271
CF/PA66	60	307

2.2 Small Scale Flexural Test

Small scale flexural tests were performed on flat coupons to characterize mechanical properties of investigated materials and to identify most-promising stacking sequences. To manufacture coupons, composite tapes were first manually laid-down into a mold according to the desired stacking sequences. The stacks were then compression molded into rectangular plates of 380 mm x 380 mm. During the consolidation cycle, laminates were heated to the recommended processing temperature (Table 1), held at this temperature for 5 minutes and then cooled to room temperature at a rate of approximately 10°C/min. A constant pressure of 0.7 MPa (100 psi) was applied during the entire molding cycle. Coupons of 38 mm in width and 250 mm in length were then

machined using water jet equipment. An 8 mm diameter hole was machined at each end to fix the specimens into the flexural test jig. Load-displacement curves were then obtained from three-point flexural tests performed at a rate of 20 mm/min using a span of 200 mm. During these tests, specimens were clamped on each side, as shown in Figure 1.

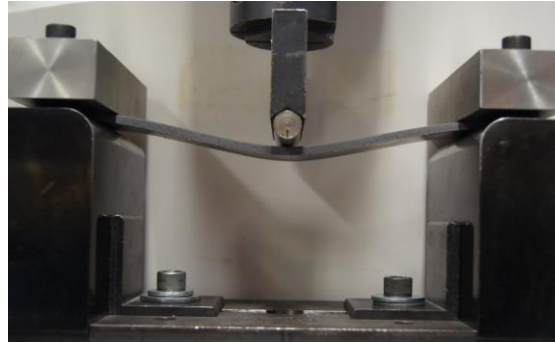


Figure 1. Three-point flexural test on rectangular coupon.

2.3 Stamping Trials

In order to perform the stamping trials, composite sheets were first manufactured. Similarly to what was described earlier for the small scale flexural tests, composite tapes were laid-down manually to the desired stacking sequences prior to being consolidated. Blanks of the proper dimensions were then cut from the consolidated sheets using water jet equipment.

During the composite stamping process, continuous fiber thermoplastic composite blanks were first heated above the melting temperature of the thermoplastic matrix in an external infrared (IR) oven and then rapidly transfer to a press where they were stamped (Figure 2a). Due to rapid cooling of the material during transfer from the oven to the press and based on previous experiences, stamping temperatures were selected to be 10 to 20°C higher than the recommended processing temperatures shown in Table 1. To prevent excessive cooling of the material prior to stamping, press closing speed of 500 mm/s was used. Forming platform used to perform the stamping trials is shown in Figure 2b.

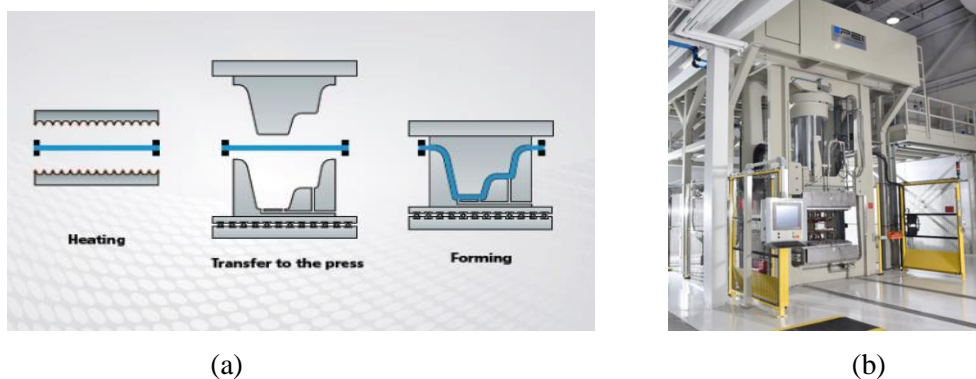


Figure 2. (a) Schematic representation of the composite stamping process and (b) NRC's stamping platform located in Boucherville.

2.4 Intrusion Beam Flexural Test

Mechanical behavior of stamped intrusion beams was investigated by performing three-point bending tests. To conduct these tests, a test jig was manufactured (Figure 3) and installed into an Instron universal frame. Experiments were conducted at a cross-head speed of 380 mm/min. From the tests, the load-displacement curves were obtained.

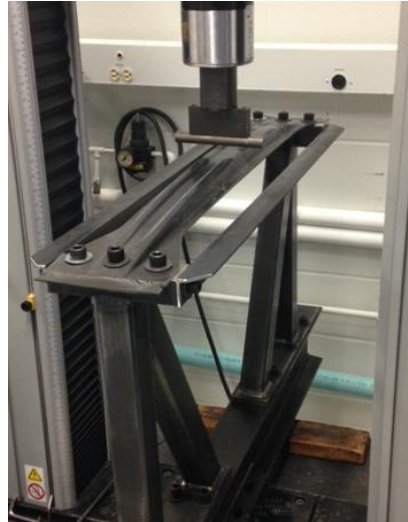


Figure 3: Flexural test on composite intrusion beam.

3 RESULTS AND DISCUSSION

3.1 Characterization of Composites Mechanical Behavior

As mentioned previously, flexural tests were performed on coupons to study the mechanical behavior of the composite materials investigated in this work. To accomplish this task, three different stacking sequences were considered for all materials, i.e. 0/90, ± 45 and quasi-isotropic (QI). A complete description of the lay-up used to perform the characterization of the mechanical behavior is provided in Table 2 for each material.

Table 2. Stacking sequences investigated for small scale tests.

Material	Stacking Sequence	Measured Thickness (mm)
GF/PP	[0/90] _{4S}	3.9
	[+45/-45] _{4S}	3.9
	[+45/-45/0/90/+45/-45/0] _S	3.9
GF/PA6	[0/90] _{3S}	3.1
	[+45/-45] _{3S}	3.3
	[0/90/+45/-45/0/90] _S	3.3
CF/PA6	[(0/90) ₅] _S	2.8
	[+45/-45] ₅ _S	2.9
	[0/90/+45/-45/0/90/+45/-45/+45/-45] _S	2.8
CF/PA66	[0/90] _{6S}	3.2
	[+45/-45] _{6S}	3.1
	[+45/-45/0/90] _{3S}	3.4

3.1.1 Glass Fiber Composites

Results of flexural tests performed on GF/PP and GF/PA6 composites are shown in Figure 4. As shown in Figure 4a, significantly different mechanical behaviors were measured for GF/PP composites depending on their stacking sequence. For GF/PP composite with ± 45 lay-up, almost linear behavior is observed up to failure. Much larger displacement at failure is also obtained for this configuration. However, lower stiffness is measured due to absence of fibers along the length of the specimens. For this material configuration also, failure occurred at the attachment point (Figure 5a) with multiple delaminations being observed at mid-span (Figure 5b). No significant change in fiber orientation could however be measured on the top and bottom surfaces of tested specimens. This suggests that large deformation was achieved through accumulation of damages in internal plies for GF/PP composite with ± 45 stacking sequence. As also shown in Figure 4a for GF/PP composites, much smaller displacements at failure were measured for the 0/90 and quasi-isotropic stacking sequences as opposed to the ± 45 stacking sequence. Only slightly higher deformation was measured for the quasi-isotropic configuration as compared to the 0/90 configuration. This can probably be attributed to the presence of ± 45 plies in the quasi-isotropic lay-up. Similar failure mode was also obtained for (0/90) and quasi-isotropic (QI) configurations. In both cases, failure was observed at mid-span (Figure 5c).

Results of flexural tests performed on GF/PA6 composites are shown in Figure 4b. As shown in this Figure, smaller displacements at failure are obtained for GF/PA6 composites as compared to those measured for GF/PP composites (Figure 4a), even if PA6 matrix can reach deformation at break of 100% and more [7]. Further study will be required to explain this behavior. For similar displacement, lower loads are also measured for GF/PA6 composites as compared to GF/PP composites. However, this can be explained by the smaller thicknesses of GF/PA6 composite laminates considered in this study as compared to those of GF/PP laminates, as shown in Table 2. Failure modes of GF/PA6 coupons are shown in Figure 6. For (0/90) specimens, failure at the attachment point was observed (Figure 6a). For ± 45 and quasi-isotropic configurations, failure at mid-span was observed.

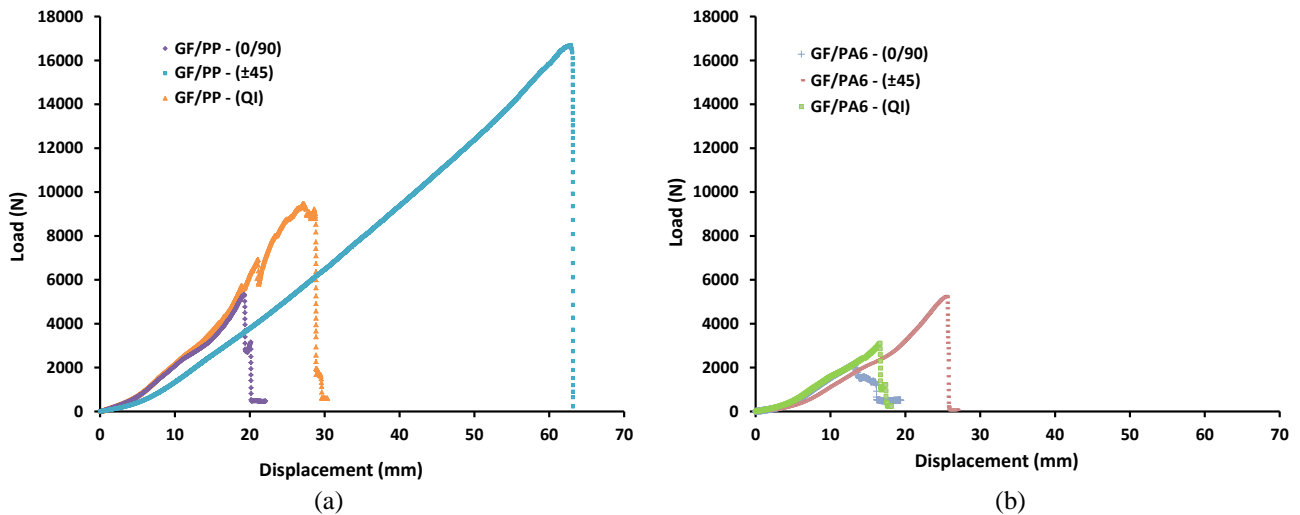


Figure 4: Load vs. displacement curves obtained for small-scale tests for (a) GF/PP laminates and (b) GF/PA6 laminates.

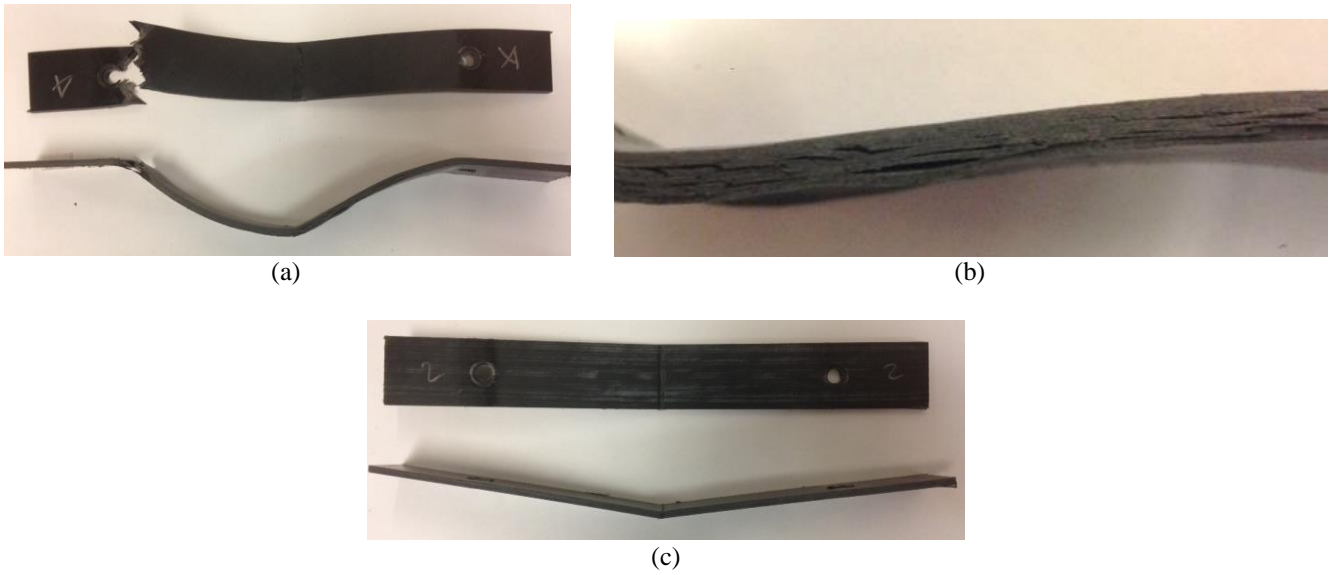


Figure 5: (a) Failure of GF/PP coupons with ± 45 lay-up, (b) delaminations in ± 45 laminate near mid-span and (c) Failure of GF/PP coupons with 0/90 lay-up.

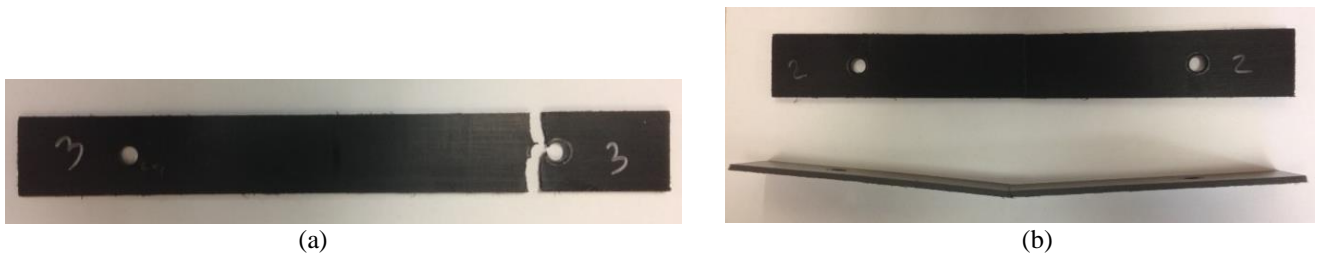


Figure 6: Failure in GF/PA6 composites: (a) 0/90 laminate and (b) quasi-isotropic laminate.

3.1.2 Carbon Fiber Composites

Results of flexural tests performed on CF/PA66 and CF/PA6 composites are shown in Figure 7. Similarly to what was observed for glass fiber composites (Figure 4), significantly different mechanical behaviors were measured for carbon fiber composites depending on polymer matrix and stacking sequences used. For CF/PA66 composites, larger deformation was obtained for composite having ± 45 lay-up (Figure 7a). However, as expected, lower stiffness was measured for this stacking sequence due to absence of fibers along the length of the specimens. For the CF/PA66 composite with ± 45 degree lay-up, failure occurred in the span of the specimens by separation of the plies at multiple interfaces (Figure 8a). Similarly to what was found for GF/PP composite (Figure 5b), multiple delaminations were also seen at mid-span. Slightly higher deformation was also measured for quasi-isotropic configuration as compared to the 0/90 configuration. This can again be attributed to the presence of ± 45 plies in quasi-isotropic lay-up. For the 0/90 and quasi-isotropic (QI) configurations, localized failures at mid-span were obtained (Figure 8b).

Results of flexural tests performed on CF/PA6 composites are shown in Figure 7b. As shown in this Figure, similar mechanical behaviours were obtained for 0/90 and quasi-isotropic configurations. As could be anticipated, much higher deformation was again obtained for the ± 45 stacking sequence. However, for that

particular stacking sequence, the displacement at failure obtained for CF/PA6 composite was seen to be significantly lower than the one measured for the CF/PA66 composite. For all CF/PA6 laminates, localized failure at mid-span was observed (Figure 9). By opposition, failure occurred by separation of plies at multiple interfaces for CF/PA66 composite with ± 45 stacking sequence (Figure 8a). This difference in failure mode probably explains the significantly different displacement at failure obtained for CF/PA66 and CF/PA6 composite having ± 45 stacking sequence.

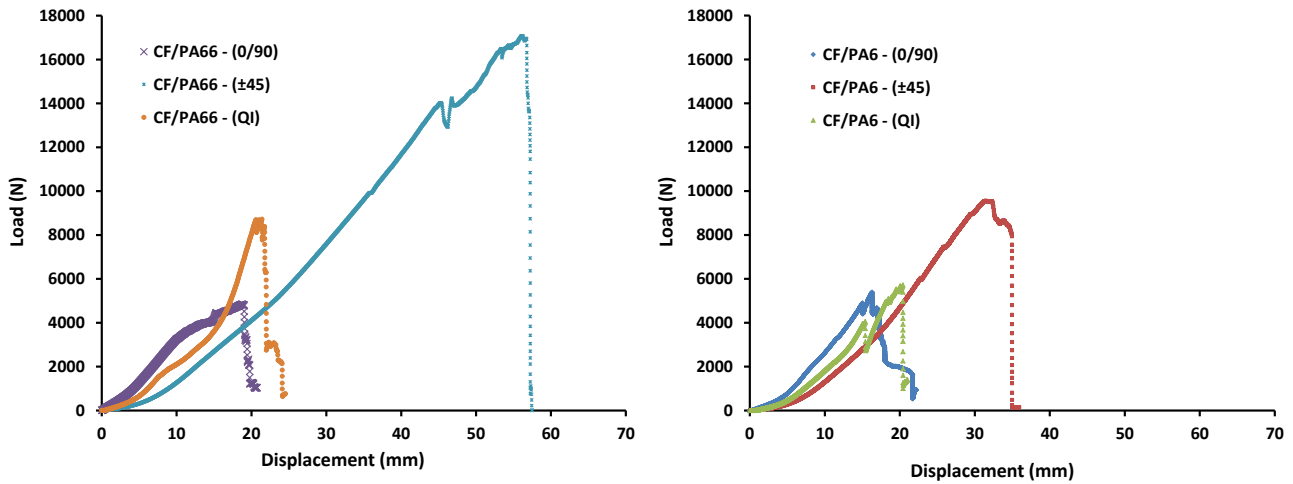


Figure 7: Load vs. displacement curves obtained for small-scale tests for (a) CF/PA6 laminates and (b) CF/PA66 laminates.

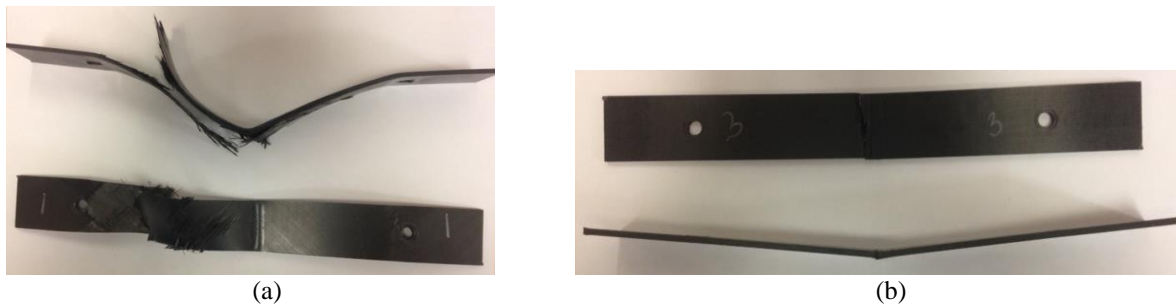


Figure 8: Failure in CF/PA66 composites: (a) ± 45 laminate and (b) 0/90 laminate.

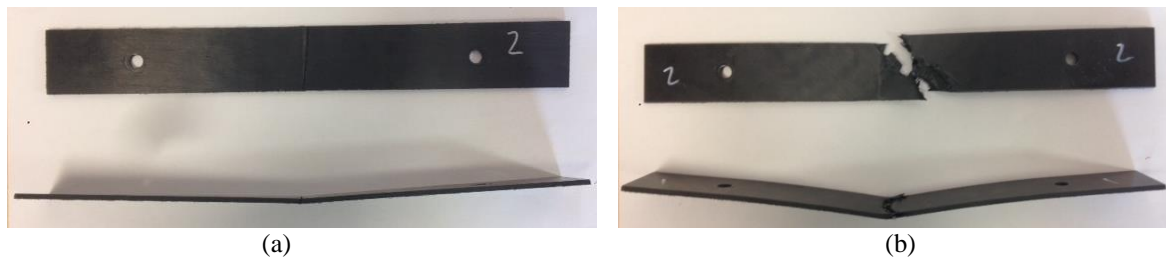


Figure 9: Failure in CF/PA6 composites: (a) 0/90 laminate and (b) ± 45 laminate.

3.2 Characterization of stamped intrusion beams

3.2.1 Requirements and Material Selection

In order to be effective, an intrusion beam must be able to sustain large deformation prior to complete failure while still providing necessary strength. As a proof of this, key requirements related to side impact protection of vehicle can be summarized as follow [6]:

- The initial crush resistance shall not be less than 2250 pounds (10 kN), where the initial crush resistance is the average force required to deform the door through the initial 6 inches (152 mm) of crush.
- The intermediate crush resistance shall not be less than 4 375 pounds (19.5 kN), where the intermediate crush resistance is the average force required to deform the door through the initial 12 inches (305 mm) of crush.
- The peak crush resistance shall not be less than 7 000 pounds (31 kN), where the peak crush resistance is the largest force required to deform the door through the entire 18 inches (457 mm) of the test.

From the results obtained on coupons (section 3.1), it can be stated that GF/PP and CF/PA66 composites have demonstrated the best potential to meet the side impact protection requirements due to their balance of strength and ability to deform significantly. These materials have thus been selected to conduct the large scale flexural tests on stamped composite intrusion beams (Figure 10). Also according to the results obtained on coupons, tests conducted on stamped intrusion beam were performed using a ± 45 stacking sequence since this configuration yielded the largest deformation.



Figure 10: Stamped thermoplastic composite intrusion beam.

3.2.2 Flexural tests on composite intrusion beam

Results of tests performed on stamped composite intrusion beams are shown in Figure 11 for GF/PP (12 plies) and CF/PA66 (20 plies) laminates. Side impact protection requirements listed in section 3.2.1 are also added to Figure 11 for comparison purposes. It is however worth mentioning that these side impact requirements are defined for an assembled door mounted on a vehicle and not for the intrusion beam itself. As shown in Figure 11, loads higher than the 10 kN, which corresponds to the initial crush resistance, were reached for a displacement of 152 mm (6 inches) for the two material investigated. Loads higher than the maximum crush

resistance were also achieved for the two materials during testing. However, beam failure was observed slightly before reaching intermediate crush distance of 305 mm. However, as mentioned previously, side protection requirements are defined for full vehicle testing. In practice, deformation of car structure will also contribute to achieving larger deformation at the door level. Therefore, results obtained can be considered very promising. Specimen failure was observed near the attachment points for GF/PP and CF/PA66 composites. Picture of failed GF/PP specimens is shown in Figure 12.

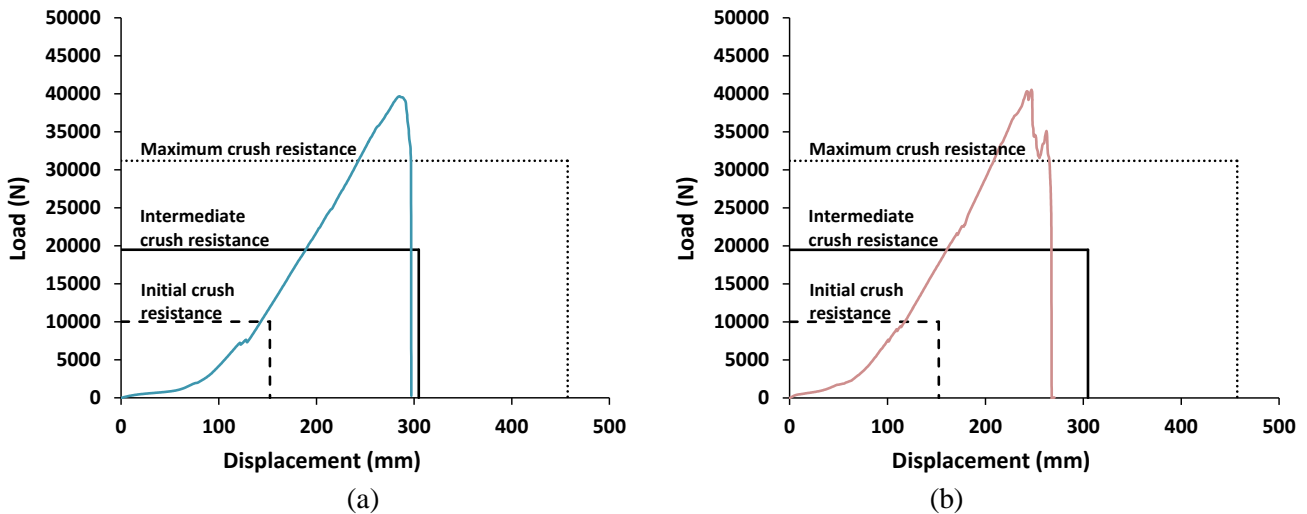


Figure 11: Load vs. displacement curves obtained on stamped composite intrusion beams for (a) GF/PP and (b) CF/PA66 laminates.



Figure 12: Failure of stamped GF/PP intrusion beam.

4 CONCLUSION

An experimental investigation was performed to evaluate the potential of thermoplastic composites to be used for the fabrication of composite intrusion beam using the composite stamping process. To assess the potential of the technology, mechanical properties of several high performance thermoplastic composite materials were first determined on coupons. From these tests, GF/PP and CF/PA66 laminates were identified as most-promising materials due to the balance of strength and deformation obtained. Several stacking sequences were also studied, i.e. 0/90, ± 45 and quasi-isotropic. Without surprise, higher displacements at failure were obtained for ± 45 laminates. Multiple delaminations were observed at mid-span, but no significant change in fiber orientation was measured for this material configuration. This suggests that large deformation was achieved through

accumulation of damages in internal plies for ± 45 composites. Stamped composite components were then manufactured from GF/PP and CF/PA66 laminates and tested under three-point flexural loading. A ± 45 stacking sequence was used to performed these tests. Load-displacement curves obtained for stamped intrusion beam were then compared to requirements for side impact protection. Results showed that sufficient strength could be achieved, but that further improvements could be required to improve displacement at failure. From these results, it can be concluded that stamping of thermoplastic composites is a very promising technology for the fabrication of structural automotive components.

5 REFERENCES

- [1] Growth Opportunities for Composites in the North American Automotive Market, Lucintel (2016)
- [2] Composite Materials Market for Automotive by Material Type (PMC, MMC, & CMC), Application & their Sub-Components (Structural, Powertrain, Interior, Exterior, & Others), Vehicle Type (PC, LCV, HCV, & Rolling Stock), & by Region-Global Forecast to 2020, Markets and Markets (October 2015)
- [3] Composite Materials Market for Automotive by Material Type (PMC, MMC, & CMC), Application & their Sub-Components (Structural, Powertrain, Interior, Exterior, & Others), Vehicle Type (PC, LCV, HCV, & Rolling Stock), & by Region-Global Forecast to 2020, Markets and Markets (October 2015)
- [4] <http://www.compositesworld.com/articles/why-cfrp>
- [5] Press forming of CETEX Continuous Fiber Reinforced Thermoplastics (TenCate).
- [6] Laboratory test Procedure for FMVSS 214S (Static), US Department of Transportation – National Highway Traffic Safety Administration.
- [7] Ultramid 8202 HS (PA6) datasheet, BASF.